

Lumen: Unleashing Versatile Vision-Centric Capabilities of Large Multimodal Models

Yang Jiao^{1,2,3*}, Shaoxiang Chen³, Zequn Jie³, Jingjing Chen^{1,2}, Lin Ma³, and Yu-Gang Jiang^{1,2}

¹ Shanghai Key Lab of Intell. Info. Processing, School of CS, Fudan University

² Shanghai Collaborative Innovation Center on Intelligent Visual Computing

³ Meituan

Abstract. Large Multimodal Model (LMM) is a hot research topic in the computer vision area and has also demonstrated remarkable potential across multiple disciplinary fields. A recent trend is to further extend and enhance the perception capabilities of LMMs. The current methods follow the paradigm of adapting the visual task outputs to the format of the language model, which is the main component of a LMM. This adaptation leads to convenient development of such LMMs with minimal modifications, however, it overlooks the intrinsic characteristics of diverse visual tasks and hinders the learning of perception capabilities. To address this issue, we propose a novel LMM architecture named **Lumen**, a **L**arge **m**ultimodal **m**odel with versatile vision-centric capability **e**nhancement. We decouple the LMM’s learning of perception capabilities into task-agnostic and task-specific stages. Lumen first promotes fine-grained vision-language concept alignment, which is the fundamental capability for various visual tasks. Thus the output of the task-agnostic stage is a shared representation for all the tasks we address in this paper. Then the task-specific decoding is carried out by flexibly routing the shared representation to lightweight task decoders with negligible training efforts. Benefiting from such a decoupled design, our Lumen surpasses existing LMM-based approaches on the COCO detection benchmark with a clear margin and exhibits seamless scalability to additional visual tasks. Furthermore, we also conduct comprehensive ablation studies and generalization evaluations for deeper insights. The code will be released at <https://github.com/SxJyJay/Lumen>.

Keywords: Large multimodal models, Vision-centric capabilities

1 Introduction

While the Large Language Models (LLMs) are currently kindling the spark of Artificial General Intelligence (AGI), Large Multimodal Models (LMMs) [35, 50, 53, 69] take a step forward by integrating visual modalities with the linguistic prowess of LLMs. With the instruction-following and content-reasoning capabilities inherited from LLMs, the LMM has successfully functioned as a versatile

* The work was done when Yang Jiao was a research intern with Meituan

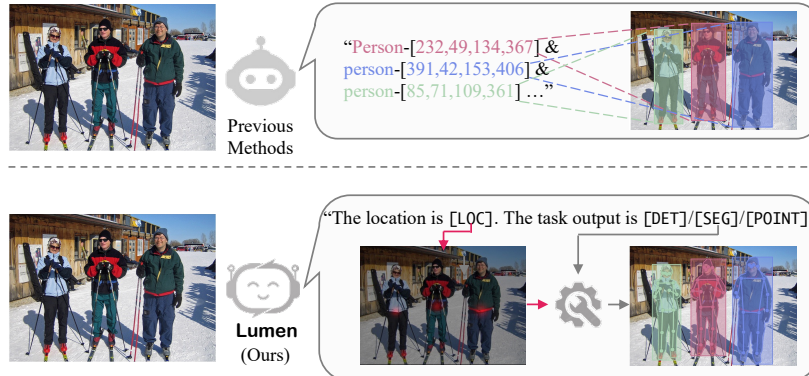


Fig. 1: The comparison of our proposed Lumen with previous methods (e.g., Griffon [65]). Previous methods serialize bounding box coordinates into discrete token sequences to conform to the language-oriented outputs format of LMMs, disregarding the unordered nature inherent in bounding boxes. Our Lumen first predicts unified heatmaps for various tasks. These heatmaps are further used for guiding simple decoding tools with the parsed task-type indicators to support versatile visual tasks. We omit the user instruction of referring to all persons in the image for conciseness.

assistant across a wide range of tasks, including visual question answering [2, 40], image captioning [21, 47], visual commonsense reasoning [3, 37], etc.

In pursuit of more convenient and efficient human-AI interaction, it is crucial to further explore fundamental vision-centric capabilities encapsulated in the LMMs, which aid in detailed object referencing and dialogue responses. Early works, e.g., MiniGPT-v2 [6], Kosmos-2 [39] and Qwen-VL [4], equip the LMM with the grounding ability by reformulating bounding boxes as a sequence of coordinate tokens and adapting them to the language model’s output space. Griffon [65] extends this design to object detection by meticulously curating a language-prompted detection dataset. Owing to such language model-oriented reformulation, these methods can be implemented with minimal modifications to existing LMMs.

Although convenient, the aforementioned approaches encounter challenges when scaling up to more intricate scenarios and vision-centric tasks. First, those LLMs highly relies on language models’s auto-regressive sequence generation method, which leads to high uncertainty when multiple objects are concurrently addressed. As shown in the first row of Fig 1, the three persons highlighted with bounding boxes of different colors lack an inherent order. And imposing a sequential order on them would exacerbate the confusion in the decoding process, as the model would be compelled to produce drastically different outputs after the same word “person”. Although sequence augmentation techniques introduced in Pix2Seq [10] can alleviate this issue, they are tailored for the object detection task and can not be seamlessly transferred to other vision-centric tasks such as instance segmentation and pose estimation. On the other hand, in contrast to tasks within the NLP field, which often exhibit stronger inter-task correlations [56], vision-centric tasks are inherently discrete due to variations in the

granularity of visual content comprehension [59]. Therefore, reformulating heterogeneous vision-centric task outputs into language-oriented formats tends to overemphasize the format consistency with language models, while the learning of the underlying visual perception capabilities and intrinsic characteristics of diverse vision tasks is overlooked.

When delving into fundamental vision-centric tasks, namely object detection, instance segmentation, and pose estimation⁴, we observe that they can be decoupled into task-agnostic and task-specific learning processes. Essentially, these tasks share a common task-agnostic objective of identifying individual instances with an instruction like “*finding the area addressed in instructions*”, while their task-specific definitions introduce different decoding rules for generating diverse formats of outputs (e.g., boxes, masks, or points). Compared with the general task-agnostic objective, task-specific outputs relies less on semantics but is more difficult for the LMMs to learn to output. Based on the above analysis, in this paper, we propose **Lumen**, a **L**arge **m**ultimodal **m**odel with vision-centric capabilities **e**nhancement, which decouples the task-agnostic and task-specific learning in two consecutive stages as shown in the Fig 1. Concretely, in the first stage, the aforementioned visual tasks are unified by reformulating them into the same matching problem. We start by feeding the user’s instruction and image into a LMM for content comprehension. The obtained responses contain a designed special token (i.e, [LOC] in Fig 1) that encapsulates the visual concepts conveyed in the provided instruction, regardless of the specific task. Subsequently, this special token interacts with image patches via a transformer-based aligner to generate a heatmap, wherein the response at each location indicates the matching probability between the instruction and the corresponding image region. In the second stage, utilizing this heatmap as indicative guidance, task-specific decoding processes are further managed by flexibly assembling predefined decoding rules and lightweight decoders to generate the final outputs with different formats. With such decoupled learning behaviors, our Lumen can concentrate on promoting fine-grained multimodal content comprehension, rather than being trapped in learning diverse specialized decoding rules lacking in semantics.

In summary, our contributions are three folds: (1) We introduce **Lumen**, a **L**arge **m**ultimodal **m**odel with vision-centric capabilities **e**nhancement, which decouples the task-agnostic and task-specific learning processes for efficiently unleashing the vision-centric potential of the LMM; (2) Our Lumen can seamlessly adapt to tasks such as object detection, instance segmentation, and pose estimation without requiring specialized dialogue datasets as done in the previous work [65]. (3) Our Lumen not only significantly outperforms existing LMM-based competitors in challenging object detection by a significant margin, but also achieves comparable performances to specialist models on several tasks, demonstrating the effectiveness of our method. Additionally, we conduct extensive ablation studies and generalization evaluations for further in-depth analysis.

⁴ We only investigate these three visual tasks in this paper, as LMMs inherently lack image generation capabilities.

2 Related Work

2.1 Large Multimodal Models (LMMs)

Benefiting from the remarkable reasoning capabilities of Large Language Models (LLMs), LMMs transfer these abilities to the vision domain by aligning visual tokens with LLMs’ input space. To achieve this, pioneering work, Flamingo [1] resamples the visual features and feeds them into attention-based adapter layers inserted in the LLM. Aiming at more comprehensive vision-language alignment, BLIP-2 [30] designs a Q-Former and jointly performs cross-modal representation learning and generative learning. Inspired by the instruction tuning technique [38, 56] in NLP field, Instruct-BLIP [13], LLaVA [35] and Mini-GPT4 [69] curate high-quality multi-modal instruction data for enhanced instruction-following abilities. However, these methods focus on high-level visual content comprehension and reasoning, ignoring the fundamental visual perception functions, such as object detection, instance segmentation, pose estimation, etc.

2.2 Vision Generalist Models

Generalist models [36, 49, 51, 52] in the vision domain aim at unifying a wide range of vision tasks using one model. Motivated by the success of sequence-to-sequence models in NLP field [47], OFA [54] and GIT [49] unify various tasks in the sequence generation format. Following this trend, Unified-IO [36], Pix2Seq v2 [11] and UniTab [63] add discrete coordinate tokens into the vocabulary, so as to accommodating more tasks. Moreover, Gato [43] successfully unifies reinforcement learning tasks as the sequence generation format. Nevertheless, the sequence generation modeling can lead to low inference speeds and degraded performances. Toward this end, Uni-Perceivers [29, 70] unify different tasks as the maximum likelihood matching problem by calculating representation similarities of all targets and each input. With such an objective, generative and non-generative tasks can be unified by selecting corresponding input and target candidates. However, these generalist models are restricted to pre-defined tasks, failing to be flexibly instructed by natural languages like LMMs.

2.3 LMMs with Vision-Centric Capabilities

To endow LMMs with vision-centric capabilities, two research directions are investigated. On the one hand, a line of work regards LLMs/LMMs as intelligent planners, and allows them to trigger a wide range of task-specific Application Program Interfaces (APIs) according to user’s instructions. HuggingGPT [46] connect GPT with a suite of visual experts. AutoGPT [61] can further execute post-processing programs after detection. Moreover, BuboGPT [66] further combines visual grounding specialists with LMMs. On the other hand, an alternative approach explores the intrinsic localization potential of LMMs with task-specific modifications. Kosmos-2 [39], MiniGPT-v2 [6], Qwen-VL [4] and Shikra [8] enlarge the vocabulary size of LMMs with discrete coordinate tokens to deal with the visual grounding task [22]. LISA [28] merges the LMM with SAM [25] for

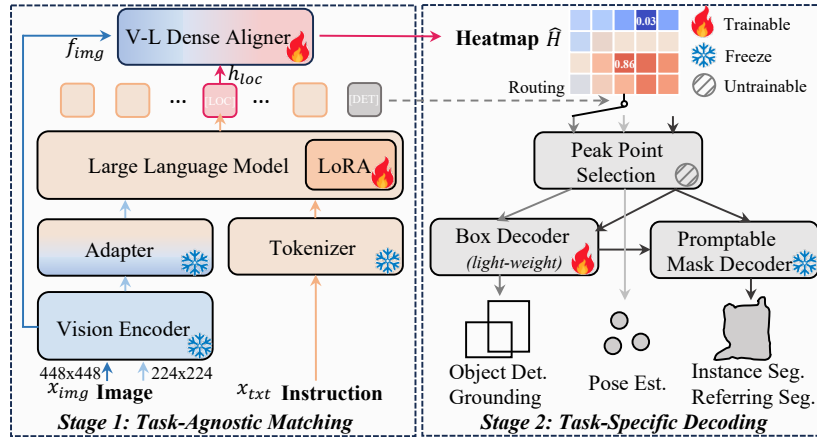


Fig. 2: The overall framework of the proposed Lumen. Our Lumen consists of two stages. In the first stage, the input image and the instruction with designed special tokens are embedded and fed into a large language model to interact and comprehend visual and textual contents. Then, the [LOC] token output and high-resolution image features are further aligned to produce a heatmap denoting cross-modal matching probabilities. In the second stage, the heatmap can serve as a strong indication for various vision tasks, and the task outputs can be obtained with lightweight task-specific decoders. The routing of the decoding pathway is determined by the task token (e.g., [DET] in image) output generated in the first stage.

enhanced reasoning capability in the referring image segmentation scenario [23]. However, these methods do not address fundamental vision tasks like object detection and instance segmentation, where multiple objects should be detected or segmented simultaneously. To address this issue, VisionLLM [55] regards an LLM as a DETR-like task decoder and customizes structural prompts for the detection task with Hungarian matching [26] for label assignment. Griffon [65] takes a different approach by leveraging the inherent detection capabilities of the LLM, introducing a language-prompted detection dataset for the instruction tuning. However, these methods leverage discrete coordinate tokens as outputs for different vision tasks, while ignoring their inherent disparities. In this paper, we disentangle the task-agnostic and task-specific learning of various vision-centric tasks to unlock the visual potential of LMMs.

3 Method

As shown in Fig 2, our proposed Lumen comprises two consecutive stages. In the first stage, we concentrate on promoting fine-grained multimodal content comprehension via densely aligning visual regions and language instructions, disregarding the discrepancies between various vision tasks. In the second stage, with the resulting alignment heatmap from the first stage, task-specific decoding is performed with specialized operations or decoders. In the following parts, we will elaborate on the detailed designs within each stage.

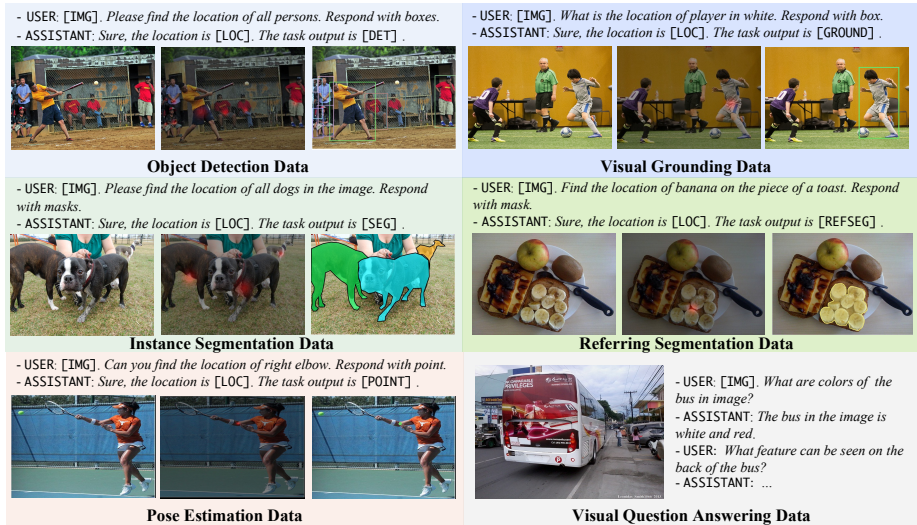


Fig. 3: The illustration of conversation data examples reformulated from different vision-centric tasks and vision-language tasks, as well as the data sample of the traditional VQA task for comparison. For each reformulated data example, we sequentially present the original image (left), the heatmap generated from annotations (middle), and the task-specific ground truth (right) in the figure.

3.1 Stage 1: Task-Agnostic Matching

Conversation Reformulation. A preliminary step for adapting vision-centric tasks to LMMs is to reformulate the visual data into conversation formats. For different tasks, we employ a unified instruction-response template: “USER: [IMG]. Please find the location of {description}. Respond with {format}. ASSISTANT: Sure, the location is [LOC]. The task output is [DET]/[SEG]/...” Here, {description} and {format} can be customized according to specific tasks. For vision-centric tasks like object detection, instance segmentation and pose estimation, {description} is a certain class name, and {format} can be boxes, masks, or points. For vision-language tasks like visual grounding and referring segmentation, {description} is the referring sentence and {format} can be boxes or masks. Apart from [IMG] that denotes image features, we also introduce a task-agnostic special token [LOC] and a set of task-specific special tokens, including [DET], [SEG], [POINT], [GROUND] and [REFSEG]. As shown in Fig 2, regardless of task types, [LOC] is tasked to summarize the visual concepts in instructions and further densely align with image regions. Task-specific tokens serve as routers for guiding the decoding pathway in the second stage. Examples of reformulated conversation data of various tasks are illustrated in Fig 3.

Model Architecture. With the given image x_{img} and reformulated instruction x_{txt} as inputs, we first feed them into a conventional LMM (LLaVA-1.1 [35] in our implementation) to generate language responses. We also extract high resolution

image features $f_{img} \in \mathbb{R}^{32 \times 32 \times 256}$ following prior works [4, 65]:

$$f_{img} = \mathcal{F}_V(x_{img}), \quad (1)$$

where \mathcal{F}_V denotes the vision encoder. Since the adopted vision encoder, CLIP-ViT [41], is pretrained to accept image inputs of 224×224 pixels, we resize its positional embeddings to adapt to higher resolution, e.g., 448×448 pixels. Afterward, the feature of [LOC] token $h_{loc} \in \mathbb{R}^{1 \times 256}$ from the generated response, together with high resolution image features, are fed into the proposed V-L dense aligner to calculate their matching probabilities, resulting in a heatmap $\hat{H} \in \mathbb{R}^{32 \times 32}$:

$$\hat{H} = \mathcal{F}_A(f_{img}, h_{loc}), \quad (2)$$

where \mathcal{F}_A represents the V-L dense aligner. In our implementation, we employ a lightweight transformer-based architecture as \mathcal{F}_A to interact high resolution image feature tokens and the [LOC] token. More discussions on the selection of architecture design are included in Sec. 4.3.

Model Training. To enrich semantics during the dense alignment, we merge data from various tasks by reformulating them into uniform conversation formats as shown in Fig 3. For various tasks, we hide diverse task-specific output format details and their learning targets are reformulated and unified as heatmaps, where each element denotes the matching probability between the instruction and the corresponding region. To construct the ground-truth heatmap H , we use a Gaussian kernel to fill the probabilities into a blank map following prior works [48, 67]:

$$H_{xy} = \exp\left(-\frac{(x - l_x)^2 + (y - l_y)^2}{2\sigma^2}\right), \quad (3)$$

where the (l_x, l_y) is the location of the one referred by the instruction, and σ is the standard deviation. For object detection and visual grounding, (l_x, l_y) is the center coordinate of each object, and σ is object size-adaptive following [67]. For instance segmentation and referring segmentation, we first convert their masks into bounding boxes by calculating enclosing rectangles of masks, and then calculate (l_x, l_y) and σ with the same rules as detection and visual grounding tasks. For pose estimation, (l_x, l_y) is the coordinate of the annotated keypoint, σ is a hyper-parameter designated as 2.

With the ground-truth heatmap H and predicted heatmap \hat{H} , we apply Gaussian focal loss following [67] as:

$$\mathcal{L}_h = -\frac{1}{N} \sum_{xy} \begin{cases} (1 - \hat{H}_{xy})^\alpha \log(\hat{H}_{xy}) & \text{if } H_{xy} = 1, \\ (1 - H_{xy})^\beta (\hat{H}_{xy})^\alpha \log(1 - \hat{H}_{xy}) & \text{otherwise.} \end{cases} \quad (4)$$

α and β are hyper-parameters of the focal loss, and N is the number of the location where the ground-truth matching probability equals to 1. We set $\alpha = 2$ and $\beta = 4$ in our implementation. For supervising the language outputs, we use

the standard cross-entropy loss \mathcal{L}_t following previous LMM-based methods [4, 65]. The overall loss function \mathcal{L} can be formulated as:

$$\mathcal{L} = \lambda_h \mathcal{L}_h + \lambda_t \mathcal{L}_t, \quad (5)$$

where λ_h and λ_t are hyper-parameters for balancing two losses. During training, since the vision encoder, adapter, tokenizer, and large language model parts in Fig 2 inherit the weights of LLaVA, we only finetune the large language model using the LoRA [19] technique and train the V-L dense aligner under the supervision of the loss function \mathcal{L} .

3.2 Stage 2: Task-Specific Decoding

Decoding Modules. We first introduce the operations of the three key modules illustrated in Fig 2. (1) **Peak point selection** parses the heatmap into a set of points, where each point indicates the center location of an identified object or keypoint. Specifically, we filter the locations with heatmap response greater than their 8 surrounding neighbors as candidate peak points, and then retain the top K candidates as the selected results. The value of K can vary across different tasks, which will be elaborated on in Sec.4.1. (2) **Box decoder** is used for further regressing the extent of the objects designated by the selected peak points. For efficiency, instead of introducing an additional network as the box decoder, we reuse the V-L dense aligner by appending two new learnable special tokens after the [LOC] token as additional text-side inputs. Accordingly, the V-L dense aligner will generate two additional 1-channel map predictions, which are used for regressing the height and width under the supervision of the L1 loss functions similar to [67]. (3) **Promptable mask decoder** can accept both points and boxes as visual instructions to generate the mask for the referred object. We directly use the SAM model [25] for executing the above process without finetuning. In general, these decoding modules introduce negligible training costs and can be easily implemented.

Decoding Pathways. On the basis of these three decoding modules, we customize their different cooperation patterns to perform diverse tasks, which will be introduced as follows: (1) **Pose estimation** requires to return the keypoint coordinates. We can easily obtain these coordinates by parsing the predicted heatmap with the peak point selection operation. (2) **Object detection** and **visual grounding** share the same output format of bounding box, therefore, we employ the identical decoding pathway for them. Specifically, as shown in Fig 2, we feed the heatmap into the cascaded peak point selection and box decoder modules to generate bounding boxes. (3) **Instance segmentation** and **referring segmentation** share a relationship analogous to the one between object detection and visual grounding, therefore, we also adopt the same decoding pathway for them. Concretely, we first parse both the center point and bounding box of the object, and then, we use them as visual instructions to guide the promptable mask decoder to generate the mask prediction.

4 Experiments

4.1 Experimental Setup

Datasets. Our training data consists of datasets from the following different tasks. (1) For object detection, we use MSCOCO [32], Objects365 [45] and OpenImages [27]. (2) For visual grounding, we use RefCOCO, RefCCO+ and RefCOCOg [64]. (3) For pose estimation, we use MSCOCO keypoints [32] and AIC [57]. (4) For visual question answering, we use LLaVA-Instruct-150k dataset [35]. It is worth noting that for instance segmentation and referring segmentation, since we first transform their masks into bounding boxes as mentioned in Sec 3.1, the constructed heatmaps are the same as the object detection. Additionally, given that we do not finetune the mask decoder in the second decoding stage, we actually do not use segmentation annotations throughout the entire training process.

Model Configurations. For the first task-agnostic matching stage, we utilize pre-trained CLIP ViT-L/14 [41] and Vicuna-7B [12] as our vision encoder and large language model, respectively.

For the second decoding stage, since the different decoding modules and pathways have been introduced in Sec 3.2, we primarily specify the K value choices and corresponding post-processing details of different tasks here. (1) For object detection and instance segmentation, which generally includes multiple objects in a given image, we set $K = 100$ to generate 100 box candidates. Then we apply regular NMS [18] to filter redundant boxes, and the remaining boxes are used for further prompt mask decoder to generate instance segmentation results. (2) For visual grounding and referring segmentation, given that only one object is referred by a referring sentence, we set $K = 1$ to only generate one predicted box/mask, and no post-processing is required. (3) For pose estimation, we follow previous works [10, 16] to first crop the single object from the image using bounding boxes. Then, for each keypoint category, we set $K = 1$ to extract the point with the highest matching probability as the prediction result.

Training Details. For object detection, visual grounding, pose estimation and visual question answering, we set their sampling rates as 0.56, 0.19, 0.19 and 0.06, respectively, for balanced data sampling. We set the batch size to 20 and train the model for 50,000 steps on 8 NVIDIA 80G A100 GPUs. The loss function balance terms λ_h and λ_t are both set to 1. We use AdamW as the optimizer with an initial learning rate of 3×10^{-4} and weight decay of 0. During training, we do not calculate heatmap loss \mathcal{L}_h for visual question answering data. We do not use any data augmentation techniques for all tasks for simplicity.

Evaluation Metrics. We adopt evaluation metrics commonly used within each field of task. For object detection and instance segmentation, we use mAP based on box IoU and mask IoU, respectively. For pose estimation, we use mAP based

Table 1: Results on fundamental vision-centric tasks and vision-language tasks. Methods in “*Vision Generalists*” adopt strong visual backbones and additional designs adaptive to vision-centric tasks. On the contrary, methods in “*LMM Generalists*” only inherit the LMM’s visual backbones, which are proficient in multimodal comprehension but weak in capturing detailed object features. This line of methods aligns with the pursuit of *unleashing the inherent vision-centric capabilities of LMMs*, rather than relying on external visual experts as proxies. We use † to indicate that the visual capabilities of VisionLLM stem from external vision encoders. “-” indicates the result is not reported or the corresponding task is not supported by the method.

Method	Object Det.			Instance Seg.			Pose Est.			Grounding	Refer Seg.
	AP	AP ₅₀	AP ₇₅	AP	AP ₅₀	AP ₇₅	AP	AP ₅₀	AP ₇₅	AP ₅₀	cIoU
<i>Task-specific Specialists</i>											
Faster R-CNN [44]	40.3	61.0	44.0	-	-	-	-	-	-	-	-
DETR [5]	43.3	63.1	45.9	-	-	-	-	-	-	-	-
Mask R-CNN [17]	41.0	61.7	44.9	37.1	58.4	40.1	-	-	-	-	-
PolarMask [58]	-	-	-	30.5	52.0	31.1	-	-	-	-	-
CPM [58]	-	-	-	-	-	-	62.7	86.2	70.9	-	-
RTMPose [20]	-	-	-	-	-	-	68.2	88.3	75.9	-	-
MDETR [24]	-	-	-	-	-	-	-	-	-	83.4	-
SeqTR [68]	-	-	-	-	-	-	-	-	-	82.7	64.7
LAVT [62]	-	-	-	-	-	-	-	-	-	-	61.2
ReLA [33]	-	-	-	-	-	-	-	-	-	-	65.0
<i>Vision Generalists</i>											
Pix2Seq-v2 [10]	46.5	-	-	38.2	-	-	64.8	-	-	-	-
Uni-Perceiver-v2 [29]	58.6	-	-	50.6	-	-	-	-	-	-	-
mPLUG-2 [60]	46.9	-	-	40.6	-	-	-	-	-	84.7	-
VisionLLM† [55]	44.6	64.0	48.1	25.1	50.0	22.4	-	-	-	-	-
<i>LMM Generalists</i>											
Shikra-7B [8]	-	-	-	-	-	-	-	-	-	82.3	-
MiniGPT-v2-7B [6]	-	-	-	-	-	-	-	-	-	84.4	-
Griffon-13B [65]	23.2	37.6	23.4	-	-	-	-	-	-	81.5	-
InstructCV [15]	-	48.5	-	-	-	-	-	-	-	-	-
Lumen-7B (Ours)	33.9	51.2	34.2	29.1	47.5	29.6	65.4	90.4	72.2	83.5	64.0

on OKS (object keypoint similarity). We implement the above metric calculation process by calling the corresponding interfaces of mmdetection [7]. For visual grounding and referring segmentation, we adopt AP₅₀ and cIoU, respectively. We implement their calculation by referring to SeqTR [68] and LISA [28].

4.2 Results on Versatile Tasks

We evaluate our method on five vision-centric and vision-language tasks as shown in Table 1. We categorize existing approaches into three groups, namely “*task-specific specialists*”, “*vision generalists*” and “*LMM generalists*”, according to their functions and architectures. Task-specific specialists are customized models in different fields. They have diverse architectural designs and are limited to a single task. Vision generalists pursue handling multiple tasks with a unified architecture. To excel in fundamental visual perception tasks, they typically uti-

lize a powerful vision encoder. LMM generalists aim to resolve every task in a conversational format. Focusing on improving the conversational quality, they adopt vision encoders proficient in multimodal content comprehension. For evaluation, we use COCO val set for both object detection and instance segmentation, COCO human body keypoints val set for pose estimation, and RefCOCOg val set for both visual grounding and referring segmentation. In the subsequent sections, we will analyze the experimental results based on the inherent characteristics of different tasks.

Object Detection & Instance Segmentation. Object detection and instance segmentation require the model to make dense predictions across the image, therefore they pose great challenges in capturing fine-grained object cues. From the results, we have the following observations: (1) Compared with other LMM generalists, our Lumen surpasses them by clear margins, achieving a 13.6 AP₅₀ boost over Griffon [65] and a 2.7 AP₅₀ boost over InstructCV [15]. This indicates the effectiveness of our method in discovering dense object cues. (2) Compared with vision generalists and task-specific specialists, our method further approaches their performances. We analyze that the performance gap might originate from two major aspects. First, we use the input size of 448×448 , which is much smaller than these competitors, for example, 1024×1024 for Pix2Seq v2 [10]. Second, we do not introduce objects decoding techniques as done in VisionLLM [55], which will be further discussed in Sec 4.3.

Pose Estimation. Following the top-down paradigm employed by previous works [10, 16], we first crop a single object from the image using the bounding box. Therefore, the pose estimation is simplified to discovering keypoints of a single object. Since the LMM generalists do not perform this task, we only compare our method with vision generalists and task-specific specialists. As illustrated in Table 1, our method outperforms the vision generalist model Pix2Seq-v2 [10] with 0.6 AP. Meanwhile, our Lumen also achieves comparable performances with task-specific specialists.

Visual Grounding & Referring Segmentation. Compared to object detection and instance segmentation, visual grounding and referring segmentation emphasize the examination of language comprehension ability, as they require the model to accurately comprehend the given sentence and then ground the referred object in the image. Here, we report the results on RefCOCOg val set for comparison because the referring expressions in it are more diverse and abundant than those in RefCOCO and RefCOCO+. As illustrated in Table 1, our method achieves better performances than Shikra [8] and Griffon [65] on visual grounding task, with AP₅₀ 83.5 vs 82.3 and 83.5 vs 81.5, respectively. Besides, our method is also comparable with the powerful MiniGPT-v2 even without meticulously crafting multi-stage training processes. These results demonstrate that our probabilistic matching design can effectively align complicated language concepts and objects in images.

Table 2: Effect of using different task combinations for training on visual grounding and object detection tasks, where we use RefCOCOg val set and COCO val set for evaluation, respectively. Both evaluation metrics are AP₅₀.

#	Object Det.	Grounding	Pose Est.	VQA	RefCOCOg	COCO
1		✓	✓	✓	72.1	25.0
2	✓			✓	24.0	39.8
3	✓	✓		✓	75.0	44.0
4	✓	✓	✓		73.6	43.3
5	✓	✓	✓	✓	73.8	43.4

4.3 Ablation Studies

For efficiency, we train models for 10,000 iterations in ablation studies by default.

Multi-task Training. We use different task combinations for training the model, and the results are shown in Table 2. Based on the results, we have the following observations: (1) Compared with adopting datasets from all tasks (#5), discarding object detection data (#1) will reduce visual grounding performances. Similarly, removing visual grounding data (#2) also results in performance degradation on object detection. This demonstrates that object detection and visual grounding can benefit from each other. (2) Excluding pose estimation data leads to performance enhancements on both visual grounding and object detection (#3 vs #5). This might be caused by the data conflict problem addressed in many generalist models [9, 55]. (3) Excluding VQA data does not significantly affect model’s performances on both detection and visual grounding, which is reasonable as VQA data do not provide explicit object-level vision-language alignment cues.

V-L Dense Aligner Architectures. We ablate different architecture design choices as shown in Table 3a, where “Conv.” indicates the operation of concatenating feature of [LOC] token with every image patch features and fusing them with two convolutional layers, and “Trans.” represents a light-weight transformer in our main method. It can be observed that substituting our transformer-based aligner with simple convolutional layers incurs significant performance degradation. This result indicates that complete vision-language interaction plays a pivotal role in dense prediction tasks like object detection, although this is less important in VQA tasks as demonstrated in LLaVA-1.5 [34].

Input Sizes. To examine the impact of various V-L dense aligner input resolutions, we resize the input image into three distinct sizes, concurrently adjusting the positional embeddings of the original CLIP ViT. As shown in Table 3b, enlarging the input size from 256×256 (default input size of CLIP ViT-L/14) to 448×448 can achieve nontrivial performance boosts. However, further increasing the size to 896×896 will harm the performances. This phenomenon indicates that excessively increasing the input size (to a scale dramatically different from its pretraining) will break the semantics of visual features, and thereby damaging the vision-language alignment.

Table 3: Ablation studies on model designs and hyper-parameters.

(a) Effect of different “V-L dense aligner” design choices. (b) Effect of different input sizes for the dense alignment. (c) Effect of different pre-trained vision encoders.

Arch.	AP	AP ₅₀	AP ₇₅	Input Size	AP	AP ₅₀	AP ₇₅	Vis Enc.	AP	AP ₅₀	AP ₇₅
Conv.	15.3	26.9	14.0	256×256	25.0	38.9	24.8	SAM ViT-H/16	12.3	20.0	12.6
Trans.	27.4	43.4	27.1	448×448	27.4	43.4	27.1	CLIP ViT-L/14	27.4	43.4	27.1
				896×896	22.3	35.2	21.8				

(d) Effect of different K value on dense pre-diction task. (e) Effect of different numbers of training iterations.

# K	20	50	100	200	#Iteration	10k	20k	30k	40k	50k
AP	25.7	26.4	27.4	26.6	AP	27.7	29.7	31.8	33.0	33.9
AP ₅₀	40.5	41.9	43.4	42.6	AP ₅₀	43.4	46.3	48.3	50.4	51.2
AP ₇₅	25.4	26.0	27.1	26.1	AP ₇₅	27.1	29.8	31.9	33.0	34.2

Vision Encoders. Since the input size can not be seamlessly scaled up as discussed above, it is worth further exploring to leverage vision encoders naturally adaptive to high-resolution image inputs. Toward this end, we employ SAM ViT-H/16 [25], which takes 1024×1024 images as inputs, as an additional vision backbone to provide high-resolution visual features for V-L dense aligner. However, as shown in Table 3c, the utilization of SAM ViT-H/16 results in a significant performance deterioration. We posit that this phenomenon can be attributed to the inadequate alignment between the SAM visual encoder and the language modality. Building upon the aforementioned experimental findings and analysis, we think that embracing vision encoders capable of processing high-resolution image inputs without compromising semantic coherence can pave the way for further enhancing the vision-centric capabilities of LMMs.

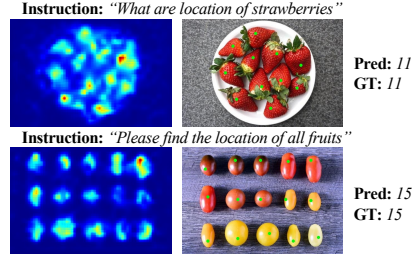
Number of K for Dense Prediction Tasks. We also investigate the impact of selecting different values for K on the dense prediction tasks, e.g., object detection. As shown in Table 3d, when K increases from 20 to 100, the model’s performance consistently improves, which can be attributed to the increased recall of true positives. However, as K further increases from 100 to 200, the model’s performance degrades slightly due to the inclusion of false positives.

Training Epochs. We record the variations in detection performance as the number of training iterations increases in Table 3e. It can be observed that the model’s performance slowly increases as the training proceeds. Due to the limitation of computational resources, we did not train our model for a longer time. The convergence speed might be limited by the optimization difficulty of utilizing a single [LOC] token to query the entire image regions. A feasible solution to mitigate this problem is to employ more special tokens like [LOC] serving as object queries in DETR [5] with the Hungarian matching for label assignment, which can accelerate training and promote performances as proved

Table 4: Generalization ability evaluation on object detection task. † indicates that VOC is not included in our training data, and thereby used for cross-dataset generalization evaluation.

Method	COCO	VOC†
RetinaNet [31]	-	77.3
Faster R-CNN [44]	-	80.4
Pix2Seq-v2 [10]	57.4	38.5
InstructCV [15]	48.5	61.7
Lumen (Ours)	51.2	78.7

Fig. 4: Qualitative results of our Lumen when generalizing to the object counting task.



in VisionLLM [55]. We do not adopt this design as it is unclear whether these tokens customized for object detection can generalize well to other tasks.

4.4 Generalization Evaluation

Generalization to Unseen Datasets. To evaluate the generalization ability of our method, we perform zero-shot evaluation on PASCAL VOC2007 val set [14]. As illustrated in Table 4, our method demonstrates superior generalization ability than other generalist models. It is worth noting that compared with InstructCV which also inherits the enormous word vocabulary of LLM, our method outperforms it on VOC zero-shot evaluation by 17.0 AP. Besides, even compared with specialist models trained on VOC dataset (i.e., RetinaNet and Faster R-CNN in Table 4), our method still achieves comparable performances.

Generalization to Unseen Tasks. To prove that the heatmap produced by our first-stage task-agnostic training is a powerful intermediate representation for scaling up to more vision-centric tasks, we apply simple decoding rules on the heatmap to make our Lumen support the object counting task [42]. Specifically, we first select 100 peak points following the operations stated in Sec 3.2. Then we filter the points with low confidence scores, and calculate the number of remaining points as the final prediction results. We illustrate user instructions, predicted heatmaps, selected points, as well as the ultimate predictions and ground-truth annotations as shown in Fig 4, where all images come from FSC-147 [42] dataset. It can be seen that our Lumen can make the correct prediction even without specifically training on the object counting task.

5 Conclusions

In this paper, we present **Lumen**, a **L**arge **m**ultimodal **m**odel with versatile vision-centric capabilities **enhancement**. Within the Lumen, we employ a decoupled design to initially promote learning task-agnostic vision-language dense alignment, and subsequently collaborate with task-specific decoding operations to address diverse tasks. Thanks to this design, our Lumen not only significantly broadens the range of visual tasks that existing LMM generalists can tackle, but also exhibits remarkable generalization capabilities to unseen datasets and tasks.

References

1. Alayrac, J.B., Donahue, J., Luc, P., Miech, A., Barr, I., Hasson, Y., Lenc, K., Mensch, A., Millican, K., Reynolds, M., et al.: Flamingo: a visual language model for few-shot learning. *Advances in Neural Information Processing Systems* **35**, 23716–23736 (2022) [4](#)
2. Antol, S., Agrawal, A., Lu, J., Mitchell, M., Batra, D., Zitnick, C.L., Parikh, D.: Vqa: Visual question answering. In: *Proceedings of the IEEE international conference on computer vision*. pp. 2425–2433 (2015) [2](#)
3. Bagherinezhad, H., Hajishirzi, H., Choi, Y., Farhadi, A.: Are elephants bigger than butterflies? reasoning about sizes of objects. In: *Proceedings of the AAAI Conference on Artificial Intelligence*. vol. 30 (2016) [2](#)
4. Bai, J., Bai, S., Yang, S., Wang, S., Tan, S., Wang, P., Lin, J., Zhou, C., Zhou, J.: Qwen-vl: A frontier large vision-language model with versatile abilities. *arXiv preprint arXiv:2308.12966* (2023) [2](#), [4](#), [7](#), [8](#)
5. Carion, N., Massa, F., Synnaeve, G., Usunier, N., Kirillov, A., Zagoruyko, S.: End-to-end object detection with transformers. In: *European conference on computer vision*. pp. 213–229. Springer (2020) [10](#), [13](#)
6. Chen, J., Zhu, D., Shen, X., Li, X., Liu, Z., Zhang, P., Krishnamoorthi, R., Chandra, V., Xiong, Y., Elhoseiny, M.: Minigpt-v2: large language model as a unified interface for vision-language multi-task learning. *arXiv preprint arXiv:2310.09478* (2023) [2](#), [4](#), [10](#)
7. Chen, K., Wang, J., Pang, J., Cao, Y., Xiong, Y., Li, X., Sun, S., Feng, W., Liu, Z., Xu, J., Zhang, Z., Cheng, D., Zhu, C., Cheng, T., Zhao, Q., Li, B., Lu, X., Zhu, R., Wu, Y., Dai, J., Wang, J., Shi, J., Ouyang, W., Loy, C.C., Lin, D.: MMDetection: Open mmlab detection toolbox and benchmark. *arXiv preprint arXiv:1906.07155* (2019) [10](#)
8. Chen, K., Zhang, Z., Zeng, W., Zhang, R., Zhu, F., Zhao, R.: Shikra: Unleashing multimodal llm’s referential dialogue magic. *arXiv preprint arXiv:2306.15195* (2023) [4](#), [10](#), [11](#)
9. Chen, S., Jie, Z., Ma, L.: Llava-mole: Sparse mixture of lora experts for mitigating data conflicts in instruction finetuning mllms. *arXiv preprint arXiv:2401.16160* (2024) [12](#)
10. Chen, T., Saxena, S., Li, L., Fleet, D.J., Hinton, G.: Pix2seq: A language modeling framework for object detection. *arXiv preprint arXiv:2109.10852* (2021) [2](#), [9](#), [10](#), [11](#), [14](#)
11. Chen, T., Saxena, S., Li, L., Lin, T.Y., Fleet, D.J., Hinton, G.E.: A unified sequence interface for vision tasks. *Advances in Neural Information Processing Systems* **35**, 31333–31346 (2022) [4](#)
12. Chiang, W.L., Li, Z., Lin, Z., Sheng, Y., Wu, Z., Zhang, H., Zheng, L., Zhuang, S., Zhuang, Y., Gonzalez, J.E., et al.: Vicuna: An open-source chatbot impressing gpt-4 with 90%* chatgpt quality. See <https://vicuna.lmsys.org> (accessed 14 April 2023) (2023) [9](#)
13. Dai, W., Li, J., Li, D., Tiong, A., Zhao, J., Wang, W., Li, B., Fung, P., Hoi, S.: Instructblip: towards general-purpose vision-language models with instruction tuning. *arxiv. Preprint posted online on June 15, 2023* (2023) [4](#)
14. Everingham, M., Van Gool, L., Williams, C.K.I., Winn, J., Zisserman, A.: The pascal visual object classes (voc) challenge. *International Journal of Computer Vision* **88**(2), 303–338 (Jun 2010) [14](#)

15. Gan, Y., Park, S., Schubert, A., Philippakis, A., Alaa, A.M.: Instructcv: Instruction-tuned text-to-image diffusion models as vision generalists. arXiv preprint arXiv:2310.00390 (2023) [10](#), [11](#), [14](#)
16. Geng, Z., Yang, B., Hang, T., Li, C., Gu, S., Zhang, T., Bao, J., Zhang, Z., Hu, H., Chen, D., et al.: Instructdiffusion: A generalist modeling interface for vision tasks. arXiv preprint arXiv:2309.03895 (2023) [9](#), [11](#)
17. He, K., Gkioxari, G., Dollár, P., Girshick, R.: Mask r-cnn. In: Proceedings of the IEEE international conference on computer vision. pp. 2961–2969 (2017) [10](#)
18. Hosang, J., Benenson, R., Schiele, B.: Learning non-maximum suppression. In: Proceedings of the IEEE conference on computer vision and pattern recognition. pp. 4507–4515 (2017) [9](#)
19. Hu, E.J., Shen, Y., Wallis, P., Allen-Zhu, Z., Li, Y., Wang, S., Wang, L., Chen, W.: Lora: Low-rank adaptation of large language models. arXiv preprint arXiv:2106.09685 (2021) [8](#)
20. Jiang, T., Lu, P., Zhang, L., Ma, N., Han, R., Lyu, C., Li, Y., Chen, K.: Rtm-pose: Real-time multi-person pose estimation based on mmpose. arXiv preprint arXiv:2303.07399 (2023) [10](#)
21. Jiao, Y., Chen, S., Jie, Z., Chen, J., Ma, L., Jiang, Y.G.: More: Multi-order relation mining for dense captioning in 3d scenes. In: European Conference on Computer Vision. pp. 528–545. Springer (2022) [2](#)
22. Jiao, Y., Jie, Z., Chen, J., Ma, L., Jiang, Y.G.: Suspected objects matter: Rethinking model’s prediction for one-stage visual grounding. In: Proceedings of the 31st ACM International Conference on Multimedia. pp. 17–26 (2023) [4](#)
23. Jiao, Y., Jie, Z., Luo, W., Chen, J., Jiang, Y.G., Wei, X., Ma, L.: Two-stage visual cues enhancement network for referring image segmentation. In: Proceedings of the 29th ACM International Conference on Multimedia. pp. 1331–1340 (2021) [5](#)
24. Kamath, A., Singh, M., LeCun, Y., Synnaeve, G., Misra, I., Carion, N.: Mdetr-modulated detection for end-to-end multi-modal understanding. In: Proceedings of the IEEE/CVF International Conference on Computer Vision. pp. 1780–1790 (2021) [10](#)
25. Kirillov, A., Mintun, E., Ravi, N., Mao, H., Rolland, C., Gustafson, L., Xiao, T., Whitehead, S., Berg, A.C., Lo, W.Y., et al.: Segment anything. arXiv preprint arXiv:2304.02643 (2023) [4](#), [8](#), [13](#)
26. Kuhn, H.W.: The hungarian method for the assignment problem. *Naval research logistics quarterly* **2**(1-2), 83–97 (1955) [5](#)
27. Kuznetsova, A., Rom, H., Alldrin, N., Uijlings, J., Krasin, I., Pont-Tuset, J., Kamali, S., Popov, S., Mallocci, M., Kolesnikov, A., et al.: The open images dataset v4: Unified image classification, object detection, and visual relationship detection at scale. *International Journal of Computer Vision* **128**(7), 1956–1981 (2020) [9](#)
28. Lai, X., Tian, Z., Chen, Y., Li, Y., Yuan, Y., Liu, S., Jia, J.: Lisa: Reasoning segmentation via large language model. arXiv preprint arXiv:2308.00692 (2023) [4](#), [10](#)
29. Li, H., Zhu, J., Jiang, X., Zhu, X., Li, H., Yuan, C., Wang, X., Qiao, Y., Wang, X., Wang, W., et al.: Uni-perceiver v2: A generalist model for large-scale vision and vision-language tasks. In: Proceedings of the IEEE/CVF Conference on Computer Vision and Pattern Recognition. pp. 2691–2700 (2023) [4](#), [10](#)
30. Li, J., Li, D., Savarese, S., Hoi, S.: Blip-2: Bootstrapping language-image pre-training with frozen image encoders and large language models. arXiv preprint arXiv:2301.12597 (2023) [4](#)

31. Lin, T.Y., Goyal, P., Girshick, R., He, K., Dollár, P.: Focal loss for dense object detection. In: Proceedings of the IEEE international conference on computer vision. pp. 2980–2988 (2017) [14](#)
32. Lin, T.Y., Maire, M., Belongie, S., Hays, J., Perona, P., Ramanan, D., Dollár, P., Zitnick, C.L.: Microsoft coco: Common objects in context. In: Computer Vision–ECCV 2014: 13th European Conference, Zurich, Switzerland, September 6–12, 2014, Proceedings, Part V 13. pp. 740–755. Springer (2014) [9](#)
33. Liu, C., Ding, H., Jiang, X.: Gres: Generalized referring expression segmentation. In: Proceedings of the IEEE/CVF Conference on Computer Vision and Pattern Recognition. pp. 23592–23601 (2023) [10](#)
34. Liu, H., Li, C., Li, Y., Lee, Y.J.: Improved baselines with visual instruction tuning. arXiv preprint arXiv:2310.03744 (2023) [12](#)
35. Liu, H., Li, C., Wu, Q., Lee, Y.J.: Visual instruction tuning. arXiv preprint arXiv:2304.08485 (2023) [1](#), [4](#), [6](#), [9](#)
36. Lu, J., Clark, C., Zellers, R., Mottaghi, R., Kembhavi, A.: Unified-io: A unified model for vision, language, and multi-modal tasks. arXiv preprint arXiv:2206.08916 (2022) [4](#)
37. Norlund, T., Hagström, L., Johansson, R.: Transferring knowledge from vision to language: How to achieve it and how to measure it? arXiv preprint arXiv:2109.11321 (2021) [2](#)
38. Ouyang, L., Wu, J., Jiang, X., Almeida, D., Wainwright, C., Mishkin, P., Zhang, C., Agarwal, S., Slama, K., Ray, A., et al.: Training language models to follow instructions with human feedback. *Advances in Neural Information Processing Systems* **35**, 27730–27744 (2022) [4](#)
39. Peng, Z., Wang, W., Dong, L., Hao, Y., Huang, S., Ma, S., Wei, F.: Kosmos-2: Grounding multimodal large language models to the world. arXiv preprint arXiv:2306.14824 (2023) [2](#), [4](#)
40. Qian, T., Chen, J., Zhuo, L., Jiao, Y., Jiang, Y.G.: Nuscenes-qa: A multi-modal visual question answering benchmark for autonomous driving scenario. arXiv preprint arXiv:2305.14836 (2023) [2](#)
41. Radford, A., Kim, J.W., Hallacy, C., Ramesh, A., Goh, G., Agarwal, S., Sastry, G., Askell, A., Mishkin, P., Clark, J., et al.: Learning transferable visual models from natural language supervision. In: International conference on machine learning. pp. 8748–8763. PMLR (2021) [7](#), [9](#)
42. Ranjan, V., Sharma, U., Nguyen, T., Hoai, M.: Learning to count everything. In: Proceedings of the IEEE/CVF Conference on Computer Vision and Pattern Recognition. pp. 3394–3403 (2021) [14](#)
43. Reed, S., Zolna, K., Parisotto, E., Colmenarejo, S.G., Novikov, A., Barth-Maron, G., Gimenez, M., Sulsky, Y., Kay, J., Springenberg, J.T., et al.: A generalist agent. arXiv preprint arXiv:2205.06175 (2022) [4](#)
44. Ren, S., He, K., Girshick, R., Sun, J.: Faster r-cnn: Towards real-time object detection with region proposal networks. *Advances in neural information processing systems* **28** (2015) [10](#), [14](#)
45. Shao, S., Li, Z., Zhang, T., Peng, C., Yu, G., Zhang, X., Li, J., Sun, J.: Objects365: A large-scale, high-quality dataset for object detection. In: Proceedings of the IEEE/CVF international conference on computer vision. pp. 8430–8439 (2019) [9](#)
46. Shen, Y., Song, K., Tan, X., Li, D., Lu, W., Zhuang, Y.: Hugginggpt: Solving ai tasks with chatgpt and its friends in huggingface. arXiv preprint arXiv:2303.17580 (2023) [4](#)

47. Vaswani, A., Shazeer, N., Parmar, N., Uszkoreit, J., Jones, L., Gomez, A.N., Kaiser, L., Polosukhin, I.: Attention is all you need. *Advances in neural information processing systems* **30** (2017) [2](#), [4](#)
48. Wang, D., Zhang, S.: Contextual instance decoupling for robust multi-person pose estimation. In: *Proceedings of the IEEE/CVF Conference on Computer Vision and Pattern Recognition*. pp. 11060–11068 (2022) [7](#)
49. Wang, J., Yang, Z., Hu, X., Li, L., Lin, K., Gan, Z., Liu, Z., Liu, C., Wang, L.: Git: A generative image-to-text transformer for vision and language. *arXiv preprint arXiv:2205.14100* (2022) [4](#)
50. Wang, J., Chen, D., Luo, C., Dai, X., Yuan, L., Wu, Z., Jiang, Y.G.: Chatvideo: A tracklet-centric multimodal and versatile video understanding system. *arXiv preprint arXiv:2304.14407* (2023) [1](#)
51. Wang, J., Chen, D., Wu, Z., Luo, C., Dai, X., Yuan, L., Jiang, Y.G.: Omnitracker: Unifying object tracking by tracking-with-detection. *arXiv preprint arXiv:2303.12079* (2023) [4](#)
52. Wang, J., Chen, D., Wu, Z., Luo, C., Zhou, L., Zhao, Y., Xie, Y., Liu, C., Jiang, Y.G., Yuan, L.: Omnivl: One foundation model for image-language and video-language tasks. *Advances in neural information processing systems* **35**, 5696–5710 (2022) [4](#)
53. Wang, J., Meng, L., Weng, Z., He, B., Wu, Z., Jiang, Y.G.: To see is to believe: Prompting gpt-4v for better visual instruction tuning. *arXiv preprint arXiv:2311.07574* (2023) [1](#)
54. Wang, P., Yang, A., Men, R., Lin, J., Bai, S., Li, Z., Ma, J., Zhou, C., Zhou, J., Yang, H.: Ofa: Unifying architectures, tasks, and modalities through a simple sequence-to-sequence learning framework. In: *International Conference on Machine Learning*. pp. 23318–23340. PMLR (2022) [4](#)
55. Wang, W., Chen, Z., Chen, X., Wu, J., Zhu, X., Zeng, G., Luo, P., Lu, T., Zhou, J., Qiao, Y., et al.: Visionllm: Large language model is also an open-ended decoder for vision-centric tasks. *arXiv preprint arXiv:2305.11175* (2023) [5](#), [10](#), [11](#), [12](#), [14](#)
56. Wei, J., Bosma, M., Zhao, V.Y., Guu, K., Yu, A.W., Lester, B., Du, N., Dai, A.M., Le, Q.V.: Finetuned language models are zero-shot learners. *arXiv preprint arXiv:2109.01652* (2021) [2](#), [4](#)
57. Wu, J., Zheng, H., Zhao, B., Li, Y., Yan, B., Liang, R., Wang, W., Zhou, S., Lin, G., Fu, Y., et al.: Ai challenger: A large-scale dataset for going deeper in image understanding. *arXiv preprint arXiv:1711.06475* (2017) [9](#)
58. Xie, E., Sun, P., Song, X., Wang, W., Liu, X., Liang, D., Shen, C., Luo, P.: Polar-mask: Single shot instance segmentation with polar representation. In: *Proceedings of the IEEE/CVF conference on computer vision and pattern recognition*. pp. 12193–12202 (2020) [10](#)
59. Xie, L., Wei, L., Zhang, X., Bi, K., Gu, X., Chang, J., Tian, Q.: Towards agi in computer vision: Lessons learned from gpt and large language models. *arXiv preprint arXiv:2306.08641* (2023) [3](#)
60. Xu, H., Ye, Q., Yan, M., Shi, Y., Ye, J., Xu, Y., Li, C., Bi, B., Qian, Q., Wang, W., et al.: mplug-2: A modularized multi-modal foundation model across text, image and video. *arXiv preprint arXiv:2302.00402* (2023) [10](#)
61. Yang, H., Yue, S., He, Y.: Auto-gpt for online decision making: Benchmarks and additional opinions. *arXiv preprint arXiv:2306.02224* (2023) [4](#)
62. Yang, Z., Wang, J., Tang, Y., Chen, K., Zhao, H., Torr, P.H.: Lavt: Language-aware vision transformer for referring image segmentation. In: *Proceedings of the IEEE/CVF Conference on Computer Vision and Pattern Recognition*. pp. 18155–18165 (2022) [10](#)

63. Yang, Z., Gan, Z., Wang, J., Hu, X., Ahmed, F., Liu, Z., Lu, Y., Wang, L.: Unitab: Unifying text and box outputs for grounded vision-language modeling. In: European Conference on Computer Vision. pp. 521–539. Springer (2022) [4](#)
64. Yu, L., Poirson, P., Yang, S., Berg, A.C., Berg, T.L.: Modeling context in referring expressions. In: Computer Vision–ECCV 2016: 14th European Conference, Amsterdam, The Netherlands, October 11–14, 2016, Proceedings, Part II 14. pp. 69–85. Springer (2016) [9](#)
65. Zhan, Y., Zhu, Y., Chen, Z., Yang, F., Tang, M., Wang, J.: Griffon: Spelling out all object locations at any granularity with large language models. arXiv preprint arXiv:2311.14552 (2023) [2](#), [3](#), [5](#), [7](#), [8](#), [10](#), [11](#)
66. Zhao, Y., Lin, Z., Zhou, D., Huang, Z., Feng, J., Kang, B.: Bubogpt: Enabling visual grounding in multi-modal llms. arXiv preprint arXiv:2307.08581 (2023) [4](#)
67. Zhou, X., Wang, D., Krähenbühl, P.: Objects as points. In: arXiv preprint arXiv:1904.07850 (2019) [7](#), [8](#)
68. Zhu, C., Zhou, Y., Shen, Y., Luo, G., Pan, X., Lin, M., Chen, C., Cao, L., Sun, X., Ji, R.: Seqtr: A simple yet universal network for visual grounding. In: Computer Vision–ECCV 2022: 17th European Conference, Tel Aviv, Israel, October 23–27, 2022, Proceedings, Part XXXV. pp. 598–615. Springer (2022) [10](#)
69. Zhu, D., Chen, J., Shen, X., Li, X., Elhoseiny, M.: Minigpt-4: Enhancing vision-language understanding with advanced large language models. arXiv preprint arXiv:2304.10592 (2023) [1](#), [4](#)
70. Zhu, X., Zhu, J., Li, H., Wu, X., Li, H., Wang, X., Dai, J.: Uni-perceiver: Pre-training unified architecture for generic perception for zero-shot and few-shot tasks. In: Proceedings of the IEEE/CVF Conference on Computer Vision and Pattern Recognition. pp. 16804–16815 (2022) [4](#)